ARTICLE

Population pharmacokinetic analysis for tisotumab vedotin in patients with locally advanced and/or metastatic solid tumors

Leonid Gibiansky[1] | **Chaitali Passey[2]** | **Jenna Voellinger[3]** | **Rudy Gunawan[3]** | **William D. Hanley[3]** | **Manish Gupta[2]** | **Helen Winter[3]**

[1]QuantPharm LLC, North Potomac, Maryland, USA

[2]Genmab, Princeton, New Jersey, USA

[3]Seagen, Bothell, Washington, USA

Correspondence
Chaitali Passey, Genmab, 777 Scudders Mill Road, Plainsboro, NJ 08536, USA.
Email: chp@genmab.com

Abstract

Tisotumab vedotin is an investigational antibody–drug conjugate (ADC) for treatment of solid tumors expressing tissue factor with accelerated approval from the US Food and Drug Administration for treatment of recurrent or metastatic cervical cancer with disease progression during or after chemotherapy. This study describes development of a population pharmacokinetic (PK) model to assess the PK profile of tisotumab vedotin and microtubule-disrupting agent monomethyl auristatin E (MMAE) using data from 399 patients with solid tumors across four phase I/II trials. The ADC–MMAE model describes ADC and MMAE concentrations following intravenous administration of tisotumab vedotin. This four-compartment model comprises a two-compartment ADC model with parallel linear and Michaelis–Menten elimination, a delay compartment, and a one-compartment MMAE model. Nonspecific linear clearance of ADC was 1.42 L/day, central volume of distribution (V_c) was 3.10 L, and median terminal half-life of ADC was 4.04 days. Apparent clearance of MMAE was 42.8 L/day, and apparent volume of distribution was 2.09 L. Terminal slope of the MMAE concentration–time curve was defined by the delay compartment rate with a half-life of 2.56 days. Patients with higher body weight and lower albumin concentration had faster ADC clearance. Male patients and those with higher body weight and lower albumin concentration had higher V_c. Body weight was the most influential covariate influencing distribution and elimination of ADC and MMAE, thus supporting weight-based dosing of tisotumab vedotin. Presence of antidrug antibodies (detected in 3.3% of patients) did not affect key PK parameters or exposures for ADC and MMAE.

Study Highlights

WHAT IS THE CURRENT KNOWLEDGE ON THE TOPIC?

Tisotumab vedotin, an antibody–drug conjugate (ADC), is being developed for treatment of solid tumors known to express tissue factor. The drug was approved by the US Food and Drug Administration in September 2021 for patients with recurrent or metastatic cervical cancer who have disease progression during or after chemotherapy; tisotumab vedotin remains investigational in other contexts.

WHAT QUESTIONS DID THIS STUDY ADDRESS?

This study describes a model that can estimate pharmacokinetic (PK) parameters of an ADC and conjugated microtubule-disrupting agent monomethyl auristatin E (MMAE), which is released following intravenous administration of tisotumab vedotin in patients with metastatic solid tumors.

WHAT DOES THIS STUDY ADD TO OUR KNOWLEDGE?

This study identifies important intrinsic and extrinsic factors affecting ADC and MMAE PKs and provides valuable PK data for tisotumab vedotin.

HOW MIGHT THIS CHANGE DRUG DISCOVERY, DEVELOPMENT, AND/OR THERAPEUTICS?

The study supports use of well-defined PK population models to describe PKs of ADCs and to estimate and summarize individual PK parameters.

INTRODUCTION

Tissue factor (TF) is a transmembrane glycoprotein that plays a key role in blood coagulation and has cell-signaling properties.[1–3] TF can induce an intracellular-signaling cascade, and its expression is enhanced in cancer via multiple pathways.[1] Expression of TF has been reported in a wide variety of tumors, including gynecologic, genitourinary, lung, prostate, pancreatic, and gastrointestinal tract cancers, as well as squamous cell carcinoma of the head and neck.[1,4–10] Overall, preclinical and translational evidence suggest that TF is a logical target for development of therapeutics for a broad range of solid tumors, potentially addressing an urgent unmet medical need for more effective and safe treatment options for these types of cancer.[11]

Tisotumab vedotin is an investigational antibody–drug conjugate (ADC) being developed for treatment of solid tumors known to express TF.[10,12,13] Tisotumab vedotin received accelerated approval from the US Food and Drug Administration in September 2021 for treatment of adult patients with recurrent or metastatic cervical cancer who have disease progression during or after chemotherapy. Structurally, tisotumab vedotin is comprised of a TF-specific, monoclonal immunoglobulin G1 (IgG1) antibody (HuMax-TF) conjugated to the clinically validated microtubule-disrupting agent monomethyl auristatin E (MMAE) using a valine–citrulline (vc) protease-cleavable linker with an average of four molecules of vc-MMAE (molecular weight, 1.25 kDa) attached to each monoclonal antibody molecule.[10,12–14] Deconjugation mainly occurs in target cells but may also occur in the circulation at

a low rate.[15] MMAE is delivered to TF-expressing cells to induce direct cytotoxicity and bystander killing of neighboring cells.[10,12,13] Treatment with tisotumab vedotin has led to tumor cell death through antibody-dependent cellular cytotoxicity, phagocytosis, and immunogenic cell death in in vitro studies.[12,13,16,17] In addition, tisotumab vedotin has demonstrated clinically meaningful and durable antitumor activity with a manageable and tolerable safety profile in several phase I/II studies for treatment of locally advanced and/or metastatic solid tumors known to express TF.[11,13,18] The pharmacokinetic (PK) profile of tisotumab vedotin was assessed in the dose-escalation phase of the first-in-human, open-label, dose-escalation/expansion innovaTV 201 phase I/II study.[11]

The present study aimed to develop population models to describe PKs of ADC and MMAE following intravenous administration of tisotumab vedotin in patients with metastatic solid tumors. Estimated population PK parameters and interindividual and intraindividual variability are also provided. Additional goals were to identify intrinsic and extrinsic covariate factors that influence distribution and elimination of ADC and MMAE and to assess effects of these covariates on PK parameters and exposure estimates.

METHODS

Analytical methods

There are three assays: one to measure ADC, one to measure unconjugated MMAE, and one to measure total

antibody (ADC plus unconjugated [free] antibody). Total antibody is not included in the population PK analysis because the concentration is similar to that of ADC, and ADC is the moiety that drives efficacy and certain safety events. Free antibody is not active and has a very small concentration. Thus, it was decided to focus on the ADC assay that is important for safety and efficacy and the MMAE assay that is important for safety. Plasma concentrations of ADC were determined using a validated enzyme-linked immunosorbent assay. Lower limit of quantification for ADC was 0.06 µg/ml. Plasma concentrations of MMAE were determined using a validated liquid chromatography method with tandem mass spectrometric detection. Lower limit of quantification for MMAE was 0.025 ng/ml. The antidrug antibodies (ADAs) to tisotumab vedotin were detected in serum samples using a validated bridging enzyme-linked immunosorbent assay. Detection limit of the screening ADA assay was 3.05 ng/ml of a surrogate anti-tisotumab vedotin antibody in the presence of tisotumab vedotin 50 µg/ml. For study NCT03485209, detection limit of the screening ADA assay was 25 ng/ml of a surrogate anti-tisotumab vedotin antibody in the presence of tisotumab vedotin 100 µg/ml.

Software

Population PK analysis was conducted via nonlinear mixed-effects modeling with NONMEM, version 7.4.3 (ICON Development Solutions). Model-based simulations were performed using a combination of R version 3.6.1 (R project; http://www.r-project.org/) for Windows (Microsoft) and NONMEM.

Population pharmacokinetic database

Data from four studies were used in the population PK analysis: NCT02001623 (innovaTV 201), NCT02552121 (innovaTV 202), NCT03438396 (innovaTV 204), and NCT03485209 (innovaTV 207). NCT02001623 is an open-label, dose-escalation/expansion phase I/II trial of 195 patients with locally advanced and/or metastatic solid tumors known to express TF. Tisotumab vedotin 0.3 to 2.2 mg/kg was administered once every 3 weeks (Q3W). NCT02552121 is an open-label, dose-escalation/expansion phase I/II trial of 33 patients with locally advanced and/or metastatic solid tumors known to express TF. Tisotumab vedotin was administered on days 1, 8, and 15 of a 28-day cycle. The dosing regimen (1.2 mg/kg administered on days 1, 8, and 15 of a 28-day cycle) investigated in the expansion part of the study was modified to 2.0 mg/kg (up to a maximum of 200 mg for patients weighing ≥100 kg)

Q3W due to higher rates and grades of ocular toxicity. NCT03438396 is an open-label, single-arm phase II trial of tisotumab vedotin 2.0 mg/kg Q3W monotherapy in 101 patients with recurrent or metastatic cervical cancer with disease progression while taking or following chemotherapy with or without bevacizumab. The data cutoff date used for this study was August 22, 2019. NCT03485209 is an open-label, multicenter phase II trial in 70 patients with certain locally advanced or metastatic solid tumors who were given tisotumab vedotin 2.0 mg/kg Q3W. The data cutoff date used for this study was August 22, 2019.

Data from patients who had at least one postbaseline quantifiable ADC or MMAE concentration by the PK analysis cutoff date were included in this study. Data consisted of patient identification, dosing information, demographic characteristics, baseline laboratory values, disease characteristics, hepatic function (based on National Cancer Institute Organ Dysfunction Working Group criteria), computed creatinine clearance, renal function (based on computed creatinine clearance category), computed glomerular filtration rate, and presence of ADAs.

Pharmacokinetic model development

Development of the ADC-MMAE population PK model was sequentially performed by creating a base population two-compartment PK model of ADC followed by adding MMAE data to the model. The base ADC and ADC-MMAE models are described in detail in the Methods S1 and Figures S1 to S6. The ADC PKs were described by a two-compartment model with parallel linear and Michaelis–Menten elimination, which is often used to describe the PKs of monoclonal antibodies and ADCs. The complexity in our model lies in the modeling of the MMAE part.

The combined ADC and unconjugated MMAE model (ADC-MMAE base model) was a complex four-compartment model comprising the two-compartment ADC model (described in the previous section) with parallel linear and Michaelis–Menten elimination, a delay compartment, and a one-compartment MMAE model (Figure 1). The ADC inputs to delay and central MMAE compartments were multiplied by the drug-to-antibody ratio (MMAE-to-ADC ratio). The drug-to-antibody ratio was described as a monoexponential decay function of time after the most recent dose with the initial value of four to the lowest value of one. On average, four molecules of vc-MMAE (molecular weight, 1.25 kDa) are attached to each monoclonal antibody molecule, yielding a total average molecular weight of ~152 kDa for tisotumab vedotin.[14] Most of the input was directed to the delay compartment, whereas a small fraction of ADC nonspecific elimination was directed to the central MMAE compartment.
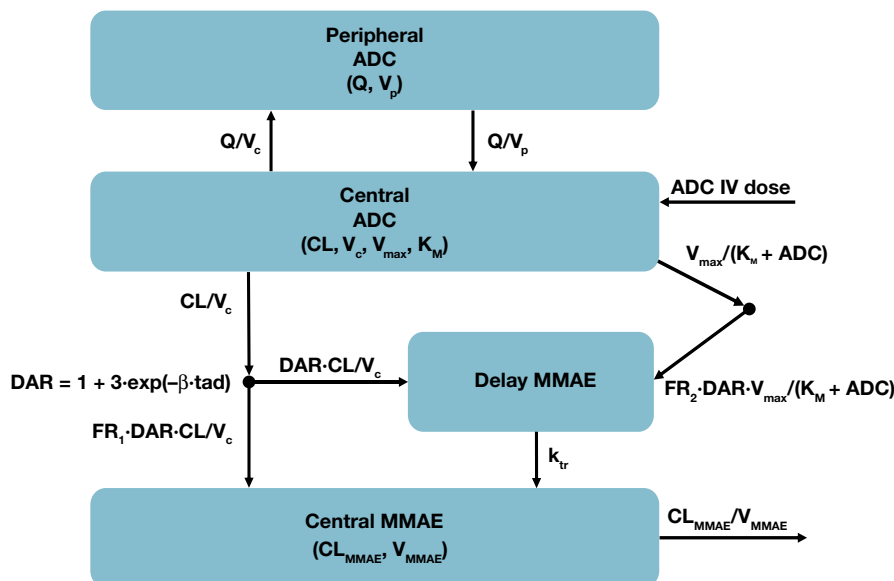
FIGURE 1 Schematic representation of the four-compartment structural ADC-MMAE model. ADC, antibody–drug conjugate; β, rate constant of drug-to-antibody ratio decay; CL, nonspecific clearance of ADC; CL_{MMAE}, apparent clearance of MMAE; DAR, drug-to-antibody ratio; FR_1, fraction of nonspecific elimination directed to the central compartment; FR_2, fraction directed to the delay compartment; IV, intravenous; K_M, Michaelis constant; k_{tr}, delay compartment rate constant; MMAE, monomethyl auristatin E; Q, intercompartmental clearance; tad, time after dose; V_c, central volume of distribution; V_{max}, maximum Michaelis–Menten elimination rate; V_{MMAE}, apparent MMAE central volume of distribution; V_p, peripheral volume of distribution.

Michaelis–Menten (target-mediated) elimination contributed a small fraction of total elimination to the delay compartment. The model code accounted for the molar ratio of ADC to MMAE and difference in mass units (ADC: µg/ml; MMAE: ng/ml) by multiplying the MMAE model prediction by the approximate molecular weight ratio of $718/152 = 4.72$. Most of the concepts implemented in the model were developed and previously tested, including a two-compartment model with linear elimination and complex three-compartment models, but this specific implementation is new due to the modeling of MMAE. All equations for the final model are provided in Table S1.

Covariate model

The full model approach was used to develop the covariate model.[19,20] Development of the covariate model followed the same pattern as that of the ADC-MMAE base model. The covariate model was first developed for the ADC model; covariates from this model were included in the ADC part of the combined ADC-MMAE covariate model; and additional covariate effects were then added to the MMAE part of the combined model. Covariates investigated in the population PK modeling are listed in Table S2. These covariate–parameter relationships were identified based on scientific interest and mechanistic plausibility. Correlations of covariates for patients in the data analysis set were graphically investigated so

that no two strongly correlated covariates were included in the full model (on the same parameter). Selection of one of the correlated covariates to include in the model was driven by mechanistic considerations and model diagnostics when testing the alternative full models that included different covariates. Covariates with low representation (missing values for >15% of patients) were not included in the full model. Additional exploratory diagnostics for the full covariate model were conducted by plotting all estimated individual random effects from the model versus covariates and by other diagnostic plots stratified by covariates of interest. When warranted by the data and existence of a plausible mechanistic explanation of the observed dependencies, additional covariates were added to the full model. Inferences about covariate effects and their clinical relevance were based on the resulting parameter estimates and measures of estimation precision (asymptotic standard errors). Specifically, interpretation and refinement of the covariate model were based on point estimates, confidence intervals (CIs), and diagnostic plots of the covariate effects. After the full model was developed, covariate effects unsupported by the data (effects close to the null value and/or with high relative standard error and/or with 95% CIs that included the null value) were excluded to arrive at the final parsimonious model. Following establishment of the final model, summaries of PK and exposure parameters by covariates of interest were used to confirm and illustrate the results. The time course of drug

exposure and distributions of the individual random effects were used to compare patients with and without detected ADAs. All parameter estimates were reported with a measure of estimation uncertainty, such as standard error of the estimates obtained from the nonlinear mixed-effects modeling covariance step.

Subanalysis

The final ADC-MMAE model (with fixed parameters) was used to analyze PK data from the Japanese innovaTV 206 study (NCT03913741). Individual PK parameters were estimated and used to compute individual exposures after 2-mg/kg Q3W doses (with no more than 200 mg/dose). Exposure values were summarized by tumor type and compared with those of non-Japanese patients included in the main analysis.

Ethics approval

All clinical studies were performed in accordance with good clinical practice guidelines from the International Council for Harmonisation of Technical Requirements for Pharmaceuticals for Human Use and the principles of the Declaration of Helsinki. Protocols were approved by appropriate institutional review boards. Written informed consent was provided by all participants.

RESULTS

Population pharmacokinetics data set

Data from 399 patients from the four clinical studies were included (Table 1). This contributed to 4847 ADC and 5145 MMAE concentrations, among which 3560 and 4901 were quantifiable concentration values for ADC and MMAE, respectively, and 1287 and 244 concentrations for ADC and MMAE, respectively, were below the limit of quantification. Observations below the limit of quantification were included in the analysis using the M3 method.[21]

Mean age of the included patients was 56.1 years; 74.2% were women; the majority (92.2%) were White; and 282 (70.7%) patients were from Europe, with the remaining 117 (29.3%) from the United States. A total of 172 (43.1%) patients had cervical cancer. Renal function was normal in 215 (53.9%) patients, mild impairment occurred in 142 (35.6%) patients, and moderate impairment occurred in 42 (10.5%) patients. No patients had severe renal impairment. Although most patients (n = 341 [85.5%]) had normal hepatic function, 58 (14.5%) had mild hepatic impairment.

No patients had moderate/severe hepatic impairment. A total of 155 (38.8%) patients had an Eastern Cooperative Oncology Group performance status (ECOG PS) of 0, and 244 (61.2%) had an ECOG PS of 1.

Pharmacokinetic properties of ADC and MMAE

The two-compartment model with parallel linear and Michaelis–Menten elimination (maximum rate [V_{max}], Michaelis constant [K_M]) provided a good fit for the ADC plasma concentration–time data. Estimates of the structural fixed-effect ADC parameters using the final ADC-MMAE model are provided in Table 2. Goodness-of-fit, interindividual random effect distribution, visual predictive check, and normalized prediction distribution error plots are provided to help judge model performance (Figures S1 to S6). The ADC nonspecific clearance (CL) value of tisotumab vedotin was determined to be 1.42 L/day, intercompartmental clearance value was 4.01 L/day, central volume of distribution (V_c) was 3.10 L, and peripheral volume of distribution (V_p) was 4.47 L. The ADC V_{max} and K_M were 3.35 µg/ml/day and 3.44 µg/ml, respectively. Following the 2-mg/kg dose, ~40% of the ADC dose was eliminated by the target-mediated route and the remaining 60% was eliminated by linear CL. Consistent with fast target-mediated elimination, K_M (3.44 µg/ml) was higher than the dissociation constant ($K_D = 0.47$ µg/ml). No accumulation of ADC during Q3W dosing was observed (Figure 2). Median terminal half-life ($t_{1/2}$) of ADC in patients included in the analysis was 4.04 (range, 2.26–7.25) days. Interindividual variability of ADC PK parameters was low (CL, 23.2%; V_c, 17.2%; V_p, 14.4%). The random effects on CL and V_c (R = 0.415) and on V_c and V_p (R = 0.586) were correlated. Intra-individual variability (residual error) of ADC PKs was also low (12.9%). Shrinkage of the random effects on CL and V_c was below 5%.

The integrated ADC-MMAE population PK model provided a good description of the PKs of MMAE. Estimates of the structural fixed-effect MMAE parameters using the final ADC-MMAE model are provided in Table 2. Apparent clearance of MMAE (CL_{MMAE}) was 42.8 L/day, and the typical value of apparent MMAE central volume of distribution (V_{MMAE}) was 2.09 L. Terminal slope of the MMAE concentration–time curve was defined by the delay compartment rate (k_{tr}) with $t_{1/2}$ ($t_{1/2,ktr} = \log(2)/k_{tr}$) of 2.56 days, a value that corresponds to steady-state (SS) volume ($V_{MMAE,SS} = CL_{MMAE}/k_{tr}$) of 158 L. Interindividual variability of MMAE PK parameters (54.7% for CL_{MMAE} and 46.3% for V_{MMAE}) was larger compared with interindividual variability of ADC PK parameters, a finding that was expected considering that MMAE is a catabolite of ADC. The random effects on CL_{MMAE} and V_{MMAE}

TABLE 1 Summary of categoric covariates

Covariate, n (%)	NCT02001623 (innovaTV 201)	NCT02552121 (innovaTV 202)	NCT03438396 (innovaTV 204)	NCT03485209 (innovaTV 207)	Total
Patients	195 (48.9)	33 (8.3)	101 (25.3)	70 (17.5)	399 (100)
Sex					
Male	55 (28.2)	4 (12.1)	—	44 (62.9)	103 (25.8)
Female	140 (71.8)	29 (87.9)	101 (100)	26 (37.1)	296 (74.2)
Race					
White	182 (93.3)	31 (93.9)	96 (95)	59 (84.3)	368 (92.2)
Black	2 (1.0)	—	1 (1.0)	3 (4.3)	6 (1.5)
Asian	5 (2.6)	2 (6.1)	2 (2.0)	1 (1.4)	10 (2.5)
Other	6 (3.1)	—	2 (2.0)	7 (10.0)	15 (3.8)
ECOG PS					
0	63 (32.3)	12 (36.4)	59 (58.4)	21 (30.0)	155 (38.8)
1	132 (67.7)	21 (63.6)	42 (41.6)	49 (70.0)	244 (61.2)
Renal impairment					
None	112 (57.4)	15 (45.5)	46 (45.5)	42 (60.0)	215 (53.9)
Mild	66 (33.8)	13 (39.4)	40 (39.6)	23 (32.9)	142 (35.6)
Moderate	17 (8.7)	5 (15.2)	15 (14.9)	5 (7.1)	42 (10.5)
Hepatic impairment					
None	167 (85.6)	25 (75.8)	93 (92.1)	56 (80.0)	341 (85.5)
Mild	28 (14.4)	8 (24.2)	8 (7.9)	14 (20.0)	58 (14.5)
Tumor type					
Cervical	57 (29.2)	14 (42.4)	101 (100)	—	172 (43.1)
Other	138 (70.8)	19 (57.6)	—	70 (100)	227 (56.9)
Region					
Europe	162 (83.1)	29 (87.9)	86 (85.1)	5 (7.1)	282 (70.7)
United States	33 (16.9)	4 (12.1)	15 (14.9)	65 (92.9)	117 (29.3)
ADA status					
Negative	189 (96.9)	33 (100)	96 (95.0)	68 (97.1)	386 (96.7)
Positive	6 (3.1)	—	5 (5.0)	2 (2.9)	13 (3.3)

Note: Data are n (%).

Abbreviations: ADA, antidrug antibody; ECOG PS, Eastern Cooperative Oncology Group performance status.

were correlated (R = 0.495). Intra-individual variability (residual error) of MMAE PKs was also higher (28.7%). Shrinkage of random effects on CL_{MMAE} and V_{MMAE} was 8% or lower. No MMAE accumulation was seen following 2-mg/kg Q3W dosing (Figure 2). The MMAE trough concentrations were predicted to be ~40 times lower than the maximum concentration (C_{max}) of MMAE. The fraction of nonspecific ADC elimination directed to the central compartment of MMAE (FR_1) was 0.0205, which was estimated with very high precision (95% CI: 0.0173–0.0237). This value appears to play an important role in the quality of fit of MMAE data. The fraction of target-mediated ADC elimination directed to the delay compartment of MMAE (FR_2) was 0.0508, which was estimated with moderate precision (95% CI: 0.0232–0.0784). This

value appears to play a limited role in the quality of fit of MMAE data. A visual predictive check for the final ADC-MMAE model is shown in Figure S4.

Comparison of simulated exposures based on population estimates of pharmacokinetic parameters

Maximum ADC concentration (C_{max}) following 2-mg/kg doses was most influenced by body weight, because it was the main contributor to interindividual variability of CL and V_c of tisotumab vedotin, with greater C_{max} in patients with higher body weight (Figure 3a). Average ADC concentration (C_{avg}) was slightly higher in patients

| Parameter	Value	RSE, %	95% CI
ADC			
CL, L/day (θ_1)	1.42	5.19	1.28–1.57
Q, L/day (θ_2)	4.01	2.93	3.78–4.24
V_c, L (θ_3)	3.10	1.23	3.03–3.18
V_p, L (θ_4)	4.47	2.30	4.27–4.68
Maximum MM elimination (V_{max}), µg/ml/day (θ_5)	3.35	11.70	2.58–4.12
Michaelis constant (K_M), µg/ml (θ_6)	3.44	12.30	2.61–4.27
SD of ADC residual error (σ_{prop}), no units (θ_7)	0.129	2.07	0.124–0.134
SD of ADC residual error (σ_{add}), µg/ml (θ_8)	0.0173	7.66	0.0147–0.0199
ADC distribution half-life ($t_{1/2,\alpha}$), day	0.28	Derived from CL, V_c, V_p, and Q	
ADC $t_{1/2}$, day	4.19		
MMAE			
Rate constant of delay (k_{tr}), 1/day (θ_9)	0.271	1.35	0.264–0.278
CL_{MMAE}, L/day (θ_{10})	42.8	7.40	36.6–49.0
V_{MMAE}, L (θ_{11})	2.09	9.82	1.69–2.50
Rate constant of DAR decay (β), 1/day (θ_{12})	0.0189	26.50	0.0091–0.0288
SD of MMAE residual error (σ_{prop}), no units (θ_{13})	0.282	2.13	0.27–0.294
SD of MMAE residual error (σ_{add}), µg/ml (θ_{14})	0.0113	4.42	0.0103–0.0123
Fraction of MMAE nonspecific elimination (FR_1, θ_{15})	0.0205	7.94	0.0173–0.0237
Fraction of MMAE target-mediated elimination (FR_2, θ_{16})	0.0508	27.7	0.0232–0.0784
MMAE delay half-life ($t_{1/2,ktr}$), day	2.56	$t_{1/2,ktr} = \log(2)/k_{tr}$	
MMAE ($t_{1/2,MMAE}$), day	0.0339	$t_{1/2,ktr} = \log(2)/K_{MMAE}$ $K_{MMAE} = CL_{MMAE}/V_{MMAE}$	

Abbreviations: ADC, antibody–drug conjugate; β, rate constant of drug-to-antibody ratio decay; CI, confidence interval; CL, nonspecific clearance of ADC; CL_{MMAE}, apparent clearance of MMAE; DAR, drug-to-antibody ratio; FR_1, fraction of nonspecific elimination directed to the central compartment; FR_2, fraction of target-mediated elimination directed to the delay compartment; K_M, Michaelis constant; K_{MMAE}, elimination rate constant of MMAE; k_{tr}, delay compartment rate constant; MM, Michaelis–Menten; MMAE, monomethyl auristatin E; PE, parameter estimate; Q, intercompartmental clearance; RSE, relative SE = 100•abs(SE/PE); σ_{add}, additive part; σ_{prop}, proportional part; $t_{1/2}$, terminal half-life; V_c, central volume of distribution; V_{max}, maximum Michaelis–Menten elimination rate; V_{MMAE}, apparent MMAE central volume of distribution; V_p, peripheral volume of distribution.

with higher body weight (Figure 4a). The model-predicted cycle 1 C_{avg} values for ADC and MMAE were compared across weight tertiles in patients who received tisotumab vedotin 2.0 mg/kg Q3W (up to a maximum of 200 mg; Figure S7). Median ADC C_{avg} values were similar across all tertiles (2.34, 2.84, and 2.99 µg/ml). CL and dose increase with weight, but dose increases faster than CL (power of 0.487), resulting in increased exposure when weight is increased. Median ADC C_{avg} was

5% higher in the third tertile of body weight and 18% lower in the first tertile compared with the middle tertile. In addition, the median predicted cycle 1 ADC C_{avg} was 2.70 µg/ml for patients weighing less than 100 kg compared with 2.72 µg/ml for patients weighing at least 100 kg with the dose maximum. The median predicted cycle 1 MMAE C_{avg} was 1.92 ng/ml for patients weighing less than 100 kg compared with 1.75 ng/ml for patients weighing at least 100 kg with the dose maximum

FIGURE 2 Predicted ADC (a) and MMAE (b) concentrations over time for tisotumab vedotin 2 mg/kg Q3W using a semi-log scale. Dark blue lines represent the median and light blue lines represent the 5th and 95th percentiles of concentration distributions. ADC, antibody–drug conjugate; MMAE, monomethyl auristatin E; Q3W, every 3 weeks.
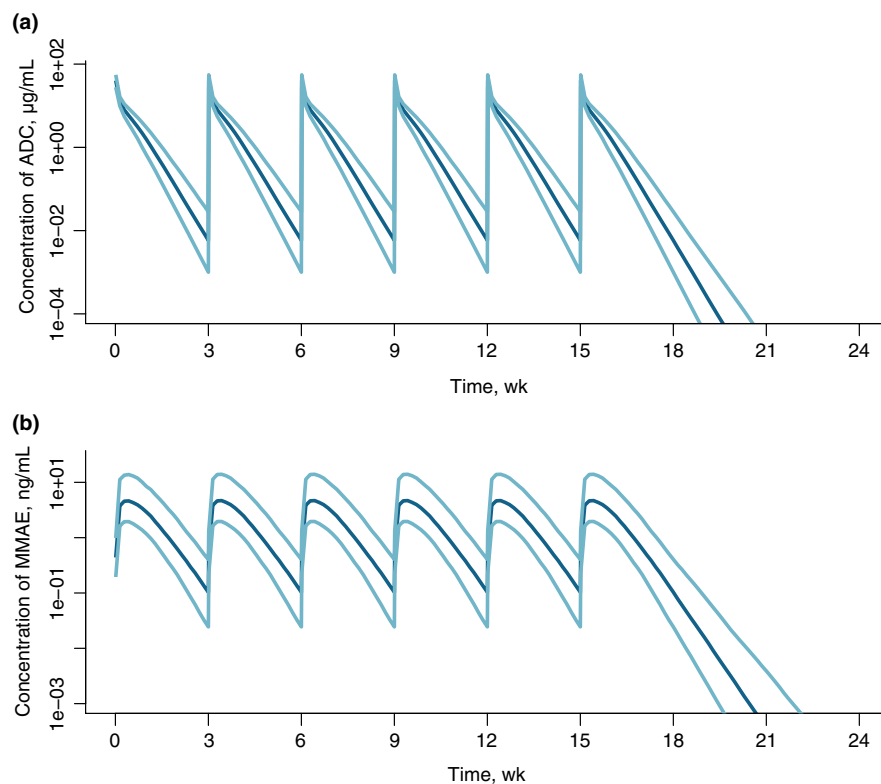
(Figure S7). Predicted ADC exposure was comparable among patients with mild hepatic impairment and those with normal function (Figure 5a) as well as among patients with renal impairment and those with normal function (Figure 5b).

Dependence of MMAE C_{max} on covariates is illustrated by Figure 3b. Tumor size had the strongest effect, with higher rates of exposure in patients with increased tumor size. Lower albumin level, an ECOG PS of 1, decreased estimated glomerular filtration rate, and mild hepatic impairment increased MMAE exposure. The MMAE C_{avg} was moderately higher in patients with increased body weight (Figure 4b). Median MMAE C_{avg} was 18% higher in the highest tertile of body weight and 15% lower in the lowest tertile compared with the middle tertile (Figure S7). Predicted MMAE exposure was 37% higher for patients with mild hepatic impairment versus normal hepatic function (Figure 5a) but comparable among patients with renal impairment and those with normal renal function (Figure 5b).

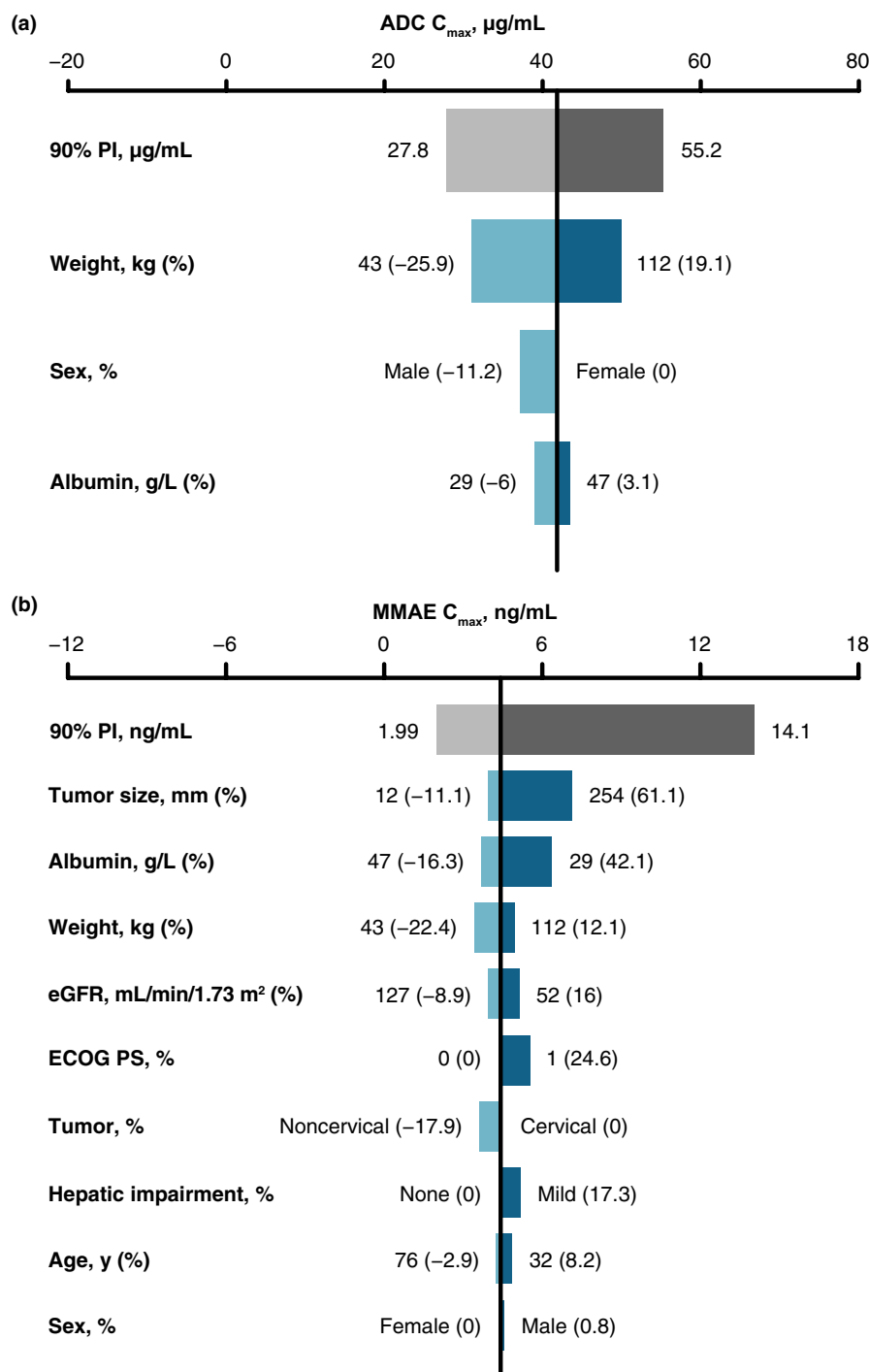## Comparison of simulated exposures based on individual empiric Bayes estimates of pharmacokinetic parameters

Exposure (area under the concentration–time curve [AUC] and C_{max}) of tisotumab vedotin was also simulated based on individual empiric Bayes estimates of PK parameters for 2-mg/kg Q3W doses and compared with covariate values, categories, or both. Among the assessed covariates, patients with increased body weight had slightly higher ADC and MMAE exposures. Patients with lower albumin concentration had slightly lower ADC exposure. Patients with lower albumin concentration had slightly higher MMAE levels, and those with high tumor burden and mild hepatic impairment had higher MMAE exposure. Other parameters assessed in this study (i.e., age, sex, renal function, ECOG PS, geographic region [Europe vs. United States]) had no clinically meaningful effect on ADC and MMAE exposures. Of 399 PK-evaluable patients from the four studies, 13 (3.3%) were positive for ADAs. The diagnostic plots for these 13 patients showed that their observed values were consistent with individual and population predictions. Comparison of individual exposures (Figures S8–S11) indicated no meaningful differences in ADC and MMAE exposures between ADA-positive and ADA-negative patients. Overall, incidence of immunogenicity was low, with no clinically meaningful effect on tisotumab vedotin PK. Simulation of exposures (AUC and C_{max}) based on individual empiric Bayes estimates of PK parameters indicated no clinically relevant impact of ADA status on ADC or MMAE exposures.

Subanalysis

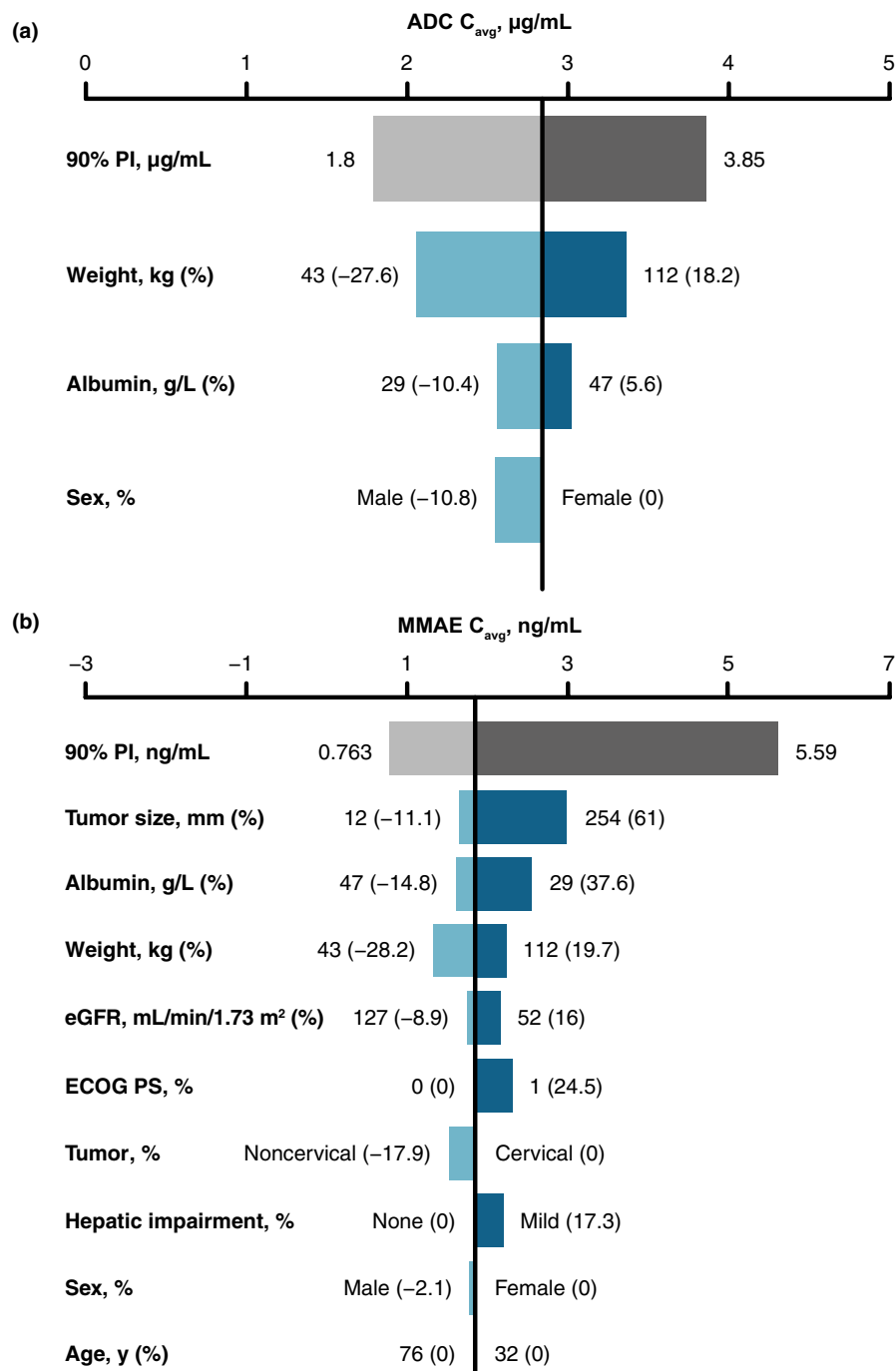Data from 18 Japanese patients with cervical cancer contributing a total of 315 ADC and 336 MMAE concentration

(a)

ADC C$_{max}$, μg/mL

−20	0	20	40	60	80

90% PI, μg/mL 27.8 55.2

Weight, kg (%) 43 (−25.9) 112 (19.1)

Sex, % Male (−11.2) Female (0)

Albumin, g/L (%) 29 (−6) 47 (3.1)

(b)

MMAE C$_{max}$, ng/mL

−12	−6	0	6	12	18

90% PI, ng/mL 1.99 14.1

Tumor size, mm (%) 12 (−11.1) 254 (61.1)

Albumin, g/L (%) 47 (−16.3) 29 (42.1)

Weight, kg (%) 43 (−22.4) 112 (12.1)

eGFR, mL/min/1.73 m² (%) 127 (−8.9) 52 (16)

ECOG PS, % 0 (0) 1 (24.6)

Tumor, % Noncervical (−17.9) Cervical (0)

Hepatic impairment, % None (0) Mild (17.3)

Age, y (%) 76 (−2.9) 32 (8.2)

Sex, % Female (0) Male (0.8)

FIGURE 3 Effect of covariates on (a) ADC C$_{max}$ (μg/ml) and (b) MMAE C$_{max}$ (ng/ml) during cycle 6 following administration of tisotumab vedotin 2 mg/kg Q3W. Baseline values for ADC and MMAE concentrations were 41.8 μg/ml and 4.4 ng/ml, respectively. The 90% PIs (shown in gray bars) correspond with the 5th and 95th percentiles of exposure distributions. For each continuous covariate (shown in blue bars), two patients were generated with extreme covariate values (2.5th and 97.5th percentiles). For each categoric covariate, one patient from each category was created; other covariates were fixed at the reference category. Lengths of each bar describe the potential impact of that particular covariate on exposure, with percentages representing change of exposure from the base. The most influential covariate is shown at the top of the plot. ADC, antibody–drug conjugate; C$_{max}$, maximum concentration; ECOG PS, Eastern Cooperative Oncology Group performance status; eGFR, estimated glomerular filtration rate; MMAE, monomethyl auristatin E; PI, prediction interval; Q3W, every 3 weeks.

values were included. Among those were 264 ADC and 326 MMAE quantifiable concentration values and 51 ADC and 10 MMAE observations below the limit of quantification. The median ADC C$_{max}$ at SS in Japanese patients was 27.9 μg/ml compared with 40.3 μg/ml in non-Japanese patients in the phase II study (NCT03438396). However, ADC C$_{avg}$, ADC AUC, and MMAE exposures were similar in Japanese and non-Japanese patients (Figure S12). The mean (range) weight of Japanese patients was 53.2 kg (30–72 kg) compared with 68.2 kg (33–110 kg) for patients with cervical cancer from the phase II study.

DISCUSSION

The four-compartment ADC-MMAE population PK model provided a good description of ADC and MMAE concentrations following intravenous administration of tisotumab vedotin in patients with various cancers. The final model indicated that patients with increased body weight and lower albumin levels had faster ADC clearance than patients with other assessed attributes. In addition, male patients, patients with higher body weight, and those with lower albumin concentration had higher

FIGURE 4 Effect of covariates on (a) ADC C_{avg} (µg/ml) and (b) MMAE C_{avg} (ng/ml) during cycle 6 following administration of tisotumab vedotin 2 mg/kg Q3W. Baseline values for ADC and MMAE concentrations were 2.8 µg/ml and 1.8 ng/ml, respectively. The 90% PIs (shown in gray bars) correspond with the 5th and 95th percentiles of exposure distributions. For each continuous covariate (shown in blue bars), two patients were generated with extreme covariate values (2.5th and 97.5th percentiles). For each categoric covariate, one patient from each category was created; other covariates were fixed at the reference category. Lengths of each bar describe the potential impact of that particular covariate on exposure, with percentages representing change of exposure from the base. The most influential covariate is shown at the top of the plot. ADC, antibody–drug conjugate; C_{avg}, average concentration; ECOG PS, Eastern Cooperative Oncology Group performance status; eGFR, estimated glomerular filtration rate; MMAE, monomethyl auristatin E; PI, prediction interval; Q3W, every 3 weeks.

ADC V_c. These covariate effects have also been observed for other ADCs, such as brentuximab vedotin and polatuzumab vedotin.[22,23] Among covariate factors that influenced distribution and elimination of ADC and MMAE, body weight was most influential. Exposure to ADC increased with body weight. Weight-based dosing for tisotumab vedotin is supported by population PK analyses, which indicate that weight-based dosing with a maximum dose of 200 mg for patients with a body weight of at least 100 kg resulted in exposures that were generally similar across tertiles of weight for both ADC and MMAE (Figure S7). Other covariates, such as age, tumor type,

mild hepatic impairment or mild/moderate renal impairment, geographic region (Europe vs. United States), and presence of ADAs, had a smaller effect not considered clinically meaningful; thus, dose adjustment to account for these covariates is not required.

The population PK subanalysis of ADC and MMAE concentrations in Japanese patients with cervical cancer revealed that the median ADC C_{max} was lower in Japanese patients compared with non-Japanese patients. However, ADC C_{max} values in Japanese patients were within the range of ADC C_{max} values in non-Japanese patients. ADC C_{avg}, ADC AUC, and MMAE exposures were similar in

(a)

(b)
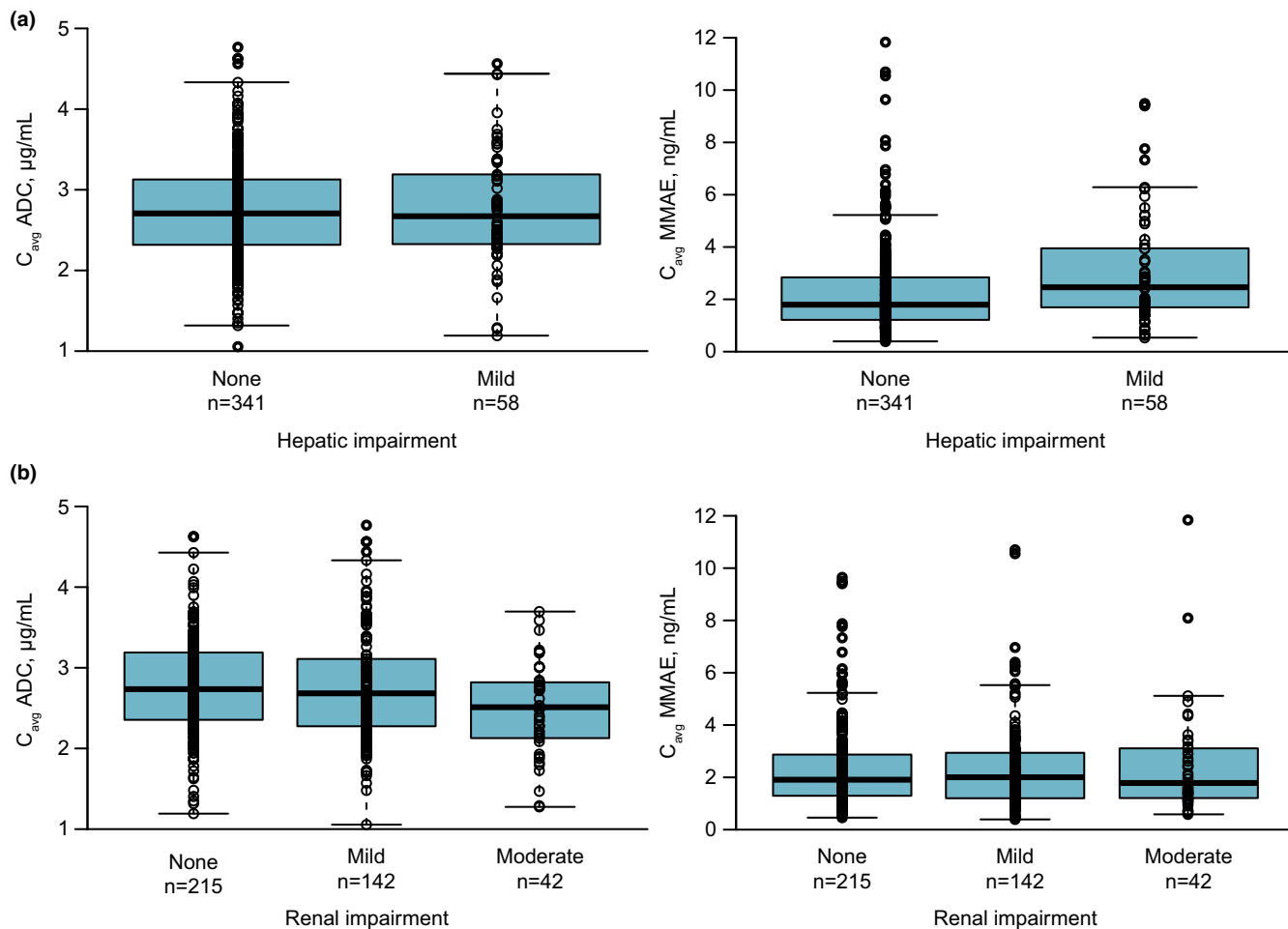
FIGURE 5 Predicted ADC and MMAE exposure in patients from the analysis data set with (a) hepatic and (b) renal impairment. ADC, antibody–drug conjugate; C_{avg}, average concentration; MMAE, monomethyl auristatin E.

Japanese and non-Japanese patients. The noted differences are likely due to differences in weight between the two populations (mean weight for the Japanese population, 53.2 kg; mean weight for the non-Japanese population, 68.2 kg), consistent with the population PK simulation results indicating a greater C_{max} in patients with higher body weight, consistent with weight-based dosing. Because exposure in the Japanese population was within the exposure range observed in the non-Japanese population, the PKs of tisotumab vedotin appears unaffected by geographic region, race, or both, and no dose adjustment is required for tisotumab vedotin based on these factors.

The estimated apparent clearance of MMAE (42.8 L/day) is similar to values reported for brentuximab vedotin in patients with CD30-expressing hematologic malignancies (55.7 L/day),[15] for polatuzumab vedotin in patients with non-Hodgkin's lymphoma (45.4 L/day),[23] and for enfortumab vedotin in patients with solid tumors (50.6 L/day).[24] However, V_{MMAE} in the current analysis (2.09 L) was much lower than the values reported for brentuximab vedotin (79.8 L)[15] and polatuzumab vedotin

(82.2 L)[23] and was attributed to differences in model structure. The $t_{1/2}$ of the MMAE concentration–time curve, defined by the half-life of the delay compartment ($t_{1/2,ktr} = 2.56$ days), corresponds to the SS volume of 158 L ($V_{MMAE,SS} = CL_{MMAE}/k_{tr}$) and is broadly similar to the SS volumes of brentuximab vedotin (108 L)[15] and polatuzumab vedotin (282 L).[23] The $t_{1/2}$ of the ADC and MMAE for tisotumab vedotin (4.04 [median] and 2.56 days, respectively) are in good agreement with values reported for enfortumab vedotin (elimination half-lives of 3.6 and 2.6 days for ADC and MMAE, respectively).[24]

Clearance of MMAE is much faster than distribution and elimination of ADC; therefore, it was expected that the kinetics of MMAE after administration of tisotumab vedotin would be formation-limited, making estimation of model parameters, except clearance, unreliable. Moreover, in the absence of data following MMAE administration, the parameters of MMAE cannot be identified because the conversion fraction of ADC to MMAE is unknown. Thus, only apparent parameters that are ratios of parameters to the true ADC-MMAE conversion fraction could be estimated.

In conclusion, the developed population PK models provide a good description of ADC and MMAE concentrations following intravenous administration of tisotumab vedotin in patients with various cancers. The final model indicated that patients with increased body weight and lower albumin concentration have faster ADC clearance; male patients, patients with increased body weight, and patients with lower albumin concentration have higher ADC V_c. These results are largely consistent with the known factors affecting the PKs of ADCs. Among covariates that influence distribution and elimination of ADC and MMAE, body weight is the most influential. With weight-proportional dosing, exposure increased with weight. In addition, exposure to MMAE was higher with large tumors. Only 3.3% of patients were positive for ADAs, and presence of ADAs did not affect key PK parameters or exposure to ADC or MMAE.

AUTHOR CONTRIBUTIONS

ACKNOWLEDGMENTS

FUNDING INFORMATION

CONFLICT OF INTEREST

REFERENCES

1. van den Berg YW, Osanto S, Reitsma PH, Versteeg HH. The relationship between tissue factor and cancer progression: insights from bench and bedside. *Blood*. 2012;119:924-932.
2. Chu AJ. Tissue factor, blood coagulation, and beyond: an overview. *Int J Inflam*. 2011;2011:1-30.
3. Kasthuri RS, Taubman MB, Mackman N. Role of tissue factor in cancer. *J Clin Oncol*. 2009;27:4834-4838.
4. Ohta S, Wada H, Nakazaki T, et al. Expression of tissue factor is associated with clinical features and angiogenesis in prostate cancer. *Anticancer Res*. 2002;22:2991-2996.
5. Akashi T, Furuya Y, Ohta S, Fuse H. Tissue factor expression and prognosis in patients with metastatic prostate cancer. *Urology*. 2003;62:1078-1082.
6. Khorana AA, Ahrendt SA, Ryan CK, et al. Tissue factor expression, angiogenesis, and thrombosis in pancreatic cancer. *Clin Cancer Res*. 2007;13:2870-2875.
7. Uno K, Homma S, Satoh T, et al. Tissue factor expression as a possible determinant of thromboembolism in ovarian cancer. *Br J Cancer*. 2007;96:290-295.
8. Yokota N, Koizume S, Miyagi E, et al. Self-production of tissue factor-coagulation factor VII complex by ovarian cancer cells. *Br J Cancer*. 2009;101:2023-2029.
9. Cocco E, Varughese J, Buza N, et al. Expression of tissue factor in adenocarcinoma and squamous cell carcinoma of the uterine cervix: implications for immunotherapy with hI-con1, a factor VII-IgGFc chimeric protein targeting tissue factor. *BMC Cancer*. 2011;11:263.
10. de Goeij BE, Satijn D, Freitag CM, et al. High turnover of tissue factor enables efficient intracellular delivery of antibody-drug conjugates. *Mol Cancer Ther*. 2015;14:1130-1140.
11. de Bono JS, Concin N, Hong DS, et al. Tisotumab vedotin in patients with advanced or metastatic solid tumours (InnovaTV 201): a first-in-human, multicentre, phase 1-2 trial. *Lancet Oncol*. 2019;20:383-393.
12. Breij EC, de Goeij BE, Verploegen S, et al. An antibody–drug conjugate that targets tissue factor exhibits potent therapeutic activity against a broad range of solid tumors. *Cancer Res*. 2014;74:1214-1226.
13. Hong DS, Concin N, Vergote I, et al. Tisotumab vedotin in previously treated recurrent or metastatic cervical cancer. *Clin Cancer Res*. 2020;26:1220-1228.
14. Tivdak. Package insert. Seagen Inc.: Bothell, WA; Genmab US, Inc.: Plainsboro, NJ; 2022.
15. Li H, Han TH, Hunder NN, Jang G, Zhao B. Population pharmacokinetics of brentuximab vedotin in patients with CD30-expressing hematologic malignancies. *J Clin Pharmacol*. 2017;57:1148-1158.
16. Alley SC, Harris JR, Cao A, et al. Tisotumab vedotin induces anti-tumor activity through MMAE-mediated, Fc-mediated, and Fab-mediated effector functions in vitro [abstract]. *Cancer Res*. 2019;79(13 suppl):221.
17. Gray E, Hensley K, Allred S, et al. Tisotumab vedotin shows immunomodulatory activity through induction of immunogenic cell death [poster 617]. Annual Meeting of the Society for Immunotherapy of Cancer, November 9–14, 2020.
18. Coleman RL, Lorusso D, Gennigens C, et al. Efficacy and safety of tisotumab vedotin in previously treated recurrent or metastatic cervical cancer (innovaTV 204/GOG-3023/ENGOT-cx6): a multicentre, open-label, single-arm, phase 2 study. *Lancet Oncol*. 2021;22:609-619.
19. Gastonguay MR. A full model estimation approach for covariate effects: inference based on clinical importance and estimation precision [abstract]. *AAPS J*. 2004;6(suppl 1):W4354.
20. Gastonguay, M.R. Full covariate models as an alternative to methods relying on statistical significance for inferences about covariate effects: a review of methodology and 42 case studies [abstract 2229]. Annual Meeting of the Population Approach Group in Europe, June 7–10, 2011.
21. Beal SL. Ways to fit a PK model with some data below the quantification limit. *J Pharmacokinet Pharmacodyn*. 2001;28:481-504.

22. Suri A, Mould DR, Liu Y, Jang G, Venkatakrishnan K. Population PK and exposure-response relationships for the antibody-drug conjugate brentuximab vedotin in CTCL patients in the phase III ALCANZA study. *Clin Pharmacol Ther.* 2018;104:989-999.

23. Lu D, Lu T, Gibiansky L, et al. Integrated two-analyte population pharmacokinetic model of polatuzumab vedotin in patients with non-Hodgkin lymphoma. *CPT Pharmacometrics Syst Pharmacol.* 2020;9:48-59.

24. Padcev. Package insert. Astellas Pharma US, Inc.: Northbrook, IL; Seagen Inc.: Bothell, WA; 2022.

SUPPORTING INFORMATION

Additional supporting information can be found online in the Supporting Information section at the end of this article.